

(V)UV degradation of the antibiotic tetracycline: Kinetics, transformation products and pathway



Dániel Krakkó^a, Bjørn Tobiassen Heieren^b, Ádám Illés^{c,d}, Kristin Kvamme^b, Sándor Dóbé^c, Gyula Záray^{a,d,*}

^a Cooperative Research Center for Environmental Sciences, Institute of Chemistry, ELTE – Eötvös Loránd University, Pázmány Péter sétány 1/A, H-1117 Budapest, Hungary

^b Faculty of Engineering and Science, Western Norway University of Applied Sciences, Inndalsveien 28, N-5063 Bergen, Norway

^c Renewable Energy Research Group, Institute of Materials and Environmental Chemistry, Research Centre for Natural Sciences, Magyar tudósok körútja 2, H-1117 Budapest, Hungary

^d Institute of Aquatic Ecology, Centre for Ecological Research, Karolina út 29-31, H-1113 Budapest, Hungary

ARTICLE INFO

Article history:

Received 1 February 2022

Received in revised form 27 April 2022

Accepted 11 May 2022

Available online 14 May 2022

Keywords:

Advanced oxidation processes

Pharmaceuticals

Persistent organic pollutants (POPs)

Contaminants of emerging concern

UV-C

VUV/UV

ABSTRACT

Tetracycline (TETR) is an antibiotic drug that is widely used in both human and veterinary medicine. It is frequently detected in activated sludge, wastewater effluent, river and lake water or sediment, usually in the pg/L – µg/L concentration range, but sometimes above the mg/L level. Conventional wastewater treatment plants have low removal efficiency for a large number of small organic molecules including TETR. Their efficiency can be increased by applying e.g., an advanced oxidation method for the post-treatment of the wastewater effluent. One possibility is the use of (V)UV lamps for simultaneous disinfection and micro-pollutant removal. In this paper, the degradation of TETR by UV ($\lambda = 254$ nm) and (V)UV ($\lambda = 185$ nm and 254 nm) light was studied, focusing on kinetics, mineralization, transformation products and degradation pathways. The effect of dissolved oxygen during irradiation was also examined. As expected, the degradation rate of TETR drastically increased in (V)UV irradiation compared to the conventional UV light. The degradation rates increased by 9% and 16% in UV and (V)UV experiments in the presence of dissolved oxygen possibly due to the generation of additional oxidative radical species. Total organic carbon removal was generally 15%, high TOC removal could only be achieved with greatly increased photon flux in (V)UV photooxidation. In total, eleven aromatic transformation products (TPs) were identified during the irradiation experiments. Three TPs (TP 418, TP 398 and TP 383) were described for the first time. The main degradation pathways include loss of water, CO, methyl or dimethylamine groups. Based on the kinetic profiles, (V)UV irradiation could effectively degrade all aromatic transformation products.

© 2022 Published by Elsevier Ltd on behalf of Institution of Chemical Engineers.
CC_BY_NC_ND_4.0

1. Introduction

Organic compounds that are resistant in varying degrees to environmental degradation through chemical, biological or photolytic processes (natural sunlight) are called persistent organic pollutants (POPs). Some POPs arise naturally in relation to volcanic activities and vegetation fires, however, most of them are from anthropogenic sources. They include pesticides, endocrine disrupting compounds, active pharmaceutical ingredients (APIs) and their metabolites,

cosmetics, industrial additives and agents, etc. In relation to human and animal health, POPs can have an additive and synergistic effect to cause endocrine disruption, cardiovascular and reproductive problems, cancer and diabetes (Alharbi et al., 2018).

APIs constitute one of the largest groups of POPs. They can be detected in surface water and wastewater globally (Aus der Beek et al., 2016). Their concentration is usually in the pg/L – µg/L range but it can also exceed mg/L (Aus der Beek et al., 2016). The long-term impact of these pharmaceuticals and their metabolites as well as their possible cocktail effects in the aquatic environment is mostly unknown (European Commission, 2019).

It has been shown that concentrations of estrogenic hormones in less than 0.1 ng/L could interfere with human, animal and wildlife reproduction (Roudbari and Rezakazemi, 2018). The possible development of antibiotic resistant genes is another major concern that

* Corresponding author at: Cooperative Research Center for Environmental Sciences, Institute of Chemistry, ELTE – Eötvös Loránd University, Pázmány Péter sétány 1/A, H-1117 Budapest, Hungary.

E-mail address: gyula.zaray@ttk.elte.hu (G. Záray).

threatens our ability to treat common infectious diseases (Guo et al., 2018; Segura et al., 2009). After consumption, APIs are not completely metabolized in the human body and are partially excreted in unchanged form, reaching wastewater treatment plants (WWTPs) through the communal sewer system. Although WWTPs aim to reduce pollution and many pollutants are completely or partially removed during conventional wastewater treatment, they are considered as important discharge points of APIs, their residues, and several other POPs with lower removal efficiency (Michael et al., 2013).

Tetracycline (TETR) is a broad-spectrum semisynthetic antibiotic drug that is used both in human and veterinary medicine. It forms part of the tetracycline antibiotic group that contains four naturally occurring molecules, namely TETR, oxytetracycline, chlortetracycline and demeclocycline as well as several semi-synthetic and synthetic compounds such as hypomicetin or doxycycline. Nowadays, TETR is used to treat infections and diseases such as acne, gonorrhoea, malaria, listeria infections, yaws, anthrax and syphilis. Chlortetracycline and oxytetracycline were widely used earlier as growth promoters in aquaculture (Yang and Carlson, 2003). However, the use of antibiotics in general as growth promoters were banned in 2006 in the European Union, and in January 2017 in the USA (Granados-Chinchilla and Rodríguez, 2017).

The extensive use of tetracycline antibiotics has led to their ubiquitous presence in the aquatic environment. They have been detected in wastewater, activated sludge, surface water and sediment, groundwater and even in drinking water (Xu et al., 2021). Adverse effects of TETR to a range of aquatic species, like the algae *Microcystis aeruginosa* and *Selenastrum capricornutum*, have been reported and there is a concern about the development of antibiotic resistant bacteria and genes (Guo et al., 2018). Because of its widespread use, TETR was also proposed as a candidate for the inclusion into the European Commission's second Watch List (Loos et al., 2018).

The removal of TETR has been widely studied in the recent decades using various treatment methods (Liu et al., 2019; Xu et al., 2021). Adsorption of TETR is an inexpensive, simple and flexible technique with many different adsorbents, such as biochar (Liu et al., 2021), graphene oxide (Ghadim et al., 2013) and reduced graphene oxide (Huizar-Félix et al., 2019), but it can only be used to concentrate TETR, not to destroy it, and it generates waste.

TETR does not degrade under visible light (Wu et al., 2020), but UV-C ($\lambda = 254$ nm) irradiation can result in a slight removal of TETR (Xu et al., 2020). The combination of H_2O_2 or Fe^{2+} (in the form of FeSO_4) with UV-C increases the removal efficiency of these AOPs (Zhao et al., 2020). Zhao et al. identified 14 different transformation products during their degradation study of TETR (Zhao et al., 2020). Luu and Lee applied UV, H_2O_2 and ozone to degrade TETR and its concentration was measured by means of a UV-Vis spectrophotometer (Luu and Lee, 2014). They have found that ozone alone and in combination with UV and/or H_2O_2 can achieve high degradation of TETR. By applying peroxomonosulfate or persulfate with UV irradiation, the generated reactive oxygenated radicals (hydroxyl radicals and $\text{SO}_4^{\cdot-}$) accelerate the degradation rate, and removal efficiencies higher than 80% can be achieved (Xu et al., 2020).

The effect of conventional UV irradiation and photocatalysis on the degradation of TETR has been widely studied. Using TiO_2 or Al_2O_3 as photocatalyst increases the degree of degradation, and the addition of H_2O_2 enhances the removal efficiency even further (Emzhina et al., 2021). The photocatalytic performance of visible light has also been investigated. Under the irradiation with wavelength of 350–800 nm, removal of TETR varied from 7% and 85% (Wu et al., 2020). Wu et al. found eight intermediate products and six more under UV irradiation ($\lambda = 350$ nm) (Wu et al., 2020). Application of black anatase- TiO_2 and N-doped TiO_2 photocatalysts showed even better results with enhanced degradation (Wu et al.,

2021). Under visible light conditions, carbon nitride can yield degrees of degradation up to 90% (Yin et al., 2021). In this study, the possible degradation pathways have been also investigated. The authors detected twelve transformation products over the $\text{Ag}_3\text{PO}_4/\text{C}_3\text{N}_5$ heterojunction (Yin et al., 2021). In recent years, metal bismuth oxide has gained much attention as a promising photocatalyst. The $\text{Bi}_2\text{WO}_6/\text{CuS}$ composites or the novel plasmonic p-n heterojunction catalyst of $\text{Ag}/\text{Ag}_6\text{Si}_2\text{O}_7/\text{Bi}_2\text{MoO}_6$ can enhance the removal efficiency up to 99% and 90%, respectively (Li et al., 2021; Mao et al., 2021).

The use of high energy vacuum UV (VUV) photons for the degradation of micropollutants has the advantage over conventional UV irradiation in that VUV photons can induce the photodissociation of water molecules, generating highly reactive hydroxyl radicals in high concentration (Krakkó et al., 2022). VUV photons can also increase degradation rates by direct photolysis. To the best of our knowledge, combined UV and VUV (referred to as (V)UV) irradiation has been previously studied once (Yao et al., 2017). In that study, the effects of solution pH, TETR concentration and the presence of Fe(II/III) ions in UV and (V)UV irradiation were examined but transformation products were not identified (Yao et al., 2017). The aim of this work was to study the effect of dissolved oxygen on the degradation and mineralization of TETR by UV and (V)UV irradiation and to identify new transformation products (TPs) and degradation pathways. Experiments were carried out in a batch photoreactor by irradiating the solutions with either a UV or a (V)UV lamp that emitted radiation at 254 nm and 254 nm + 185 nm, respectively.

2. Materials and methods

2.1. Chemicals and reagents

TETR of 94.12% purity was purchased from Alfa Aesar [Thermo Fisher (Kandel) GmbH, Karlsruhe, Germany]. Standard solutions of TETR were prepared in ultrapure water (UPW) at two concentration levels: 5×10^{-6} M and 5×10^{-5} M. UPW was produced with an ELGA Purelab Option-R7 unit (ELGA LabWater/VWS Ltd., High Wycombe, UK). LC-MS grade acetonitrile, methanol and formic acid (99% by weight) were purchased from VWR (VWR International Ltd., Debrecen, Hungary). For the irradiation experiments, high purity oxygen (99.95%), nitrogen (99.996%) and argon (99.996%) were used.

2.2. Irradiation setup

Aliquots of 650 mL of standard solutions of TETR were prepared in UPW and subjected to irradiation in a tubular batch-scale Pyrex photoreactor as described elsewhere (Krakkó et al., 2019; Krakkó et al., 2022). Briefly, two low-pressure mercury lamps were applied; a conventional germicidal UV lamp (5.4×10^{-8} molphoton $\text{cm}^{-2} \text{s}^{-1}$ photon flux at 254 nm) and a (V)UV lamp (7.6×10^{-8} and 4.6×10^{-9} molphoton $\text{cm}^{-2} \text{s}^{-1}$ photon fluxes at 254 and 185 nm, respectively). The two lamps had identical geometry that are described elsewhere (Krakkó et al., 2022). The distance between the surface of the quartz sleeve and the internal surface of the photoreactor was 24 mm. In these experiments, the effective arc length of the (V)UV lamp was reduced by covering the lamp sleeve with Pyrex glass tubes at the top and bottom to reduce the relatively high photon flux at 185 nm of the (V)UV lamp. The solutions in the photoreactor were either purged with high purity (99.996%) argon at 500 mL/min or oxygen (99.5%) at 990 mL/min during irradiation, and the lamps were cooled with high purity (99.996%) nitrogen at 800 mL/min. The pH of the solutions were 4.9–5.3 depending on the concentration of TETR (HCl salt). Experiments focusing on reaction kinetics and the identification of transformation products were carried out at 5×10^{-6} M (2.2 mg/L) TETR concentration, while 5×10^{-5} M (22.2 mg/L) was used for studying mineralization.

2.3. Analytical procedures

For the identification of TPs, irradiation experiments were stopped at predefined times, 50 mL of samples were collected and preconcentrated using 60 mg Oasis HLB solid-phase extraction cartridges (Waters Ltd., Budapest, Hungary). The steps of the solid-phase extraction are described in detail elsewhere (Krakkó et al., 2019).

Samples with and without preconcentration were measured with an ultrahigh performance liquid chromatograph coupled to a quadrupole time-of-flight high resolution mass spectrometer (Bruker Daltonik GmbH, Bremen, Germany). For the chromatographic separation, a Bruker Intensity Solo 2 C18 column (100 mm × 2.1 mm, 2 μm particle size) equipped with an Acclaim RS120 C18 guard column (10 mm × 2.1 mm, 5 μm particle size) was applied. Mobile phases were 0.1% (v/v) formic acid in UPW (eluent A) and acetonitrile (eluent B). For the quantitative analysis of TETR, isocratic elution with 20% eluent B with a run time of 2.5 min was used. For the identification of the TPs, the following gradient elution was used: 0–2 min, 10% B; 2–35 min, 90% B with 4 min long post-run equilibration time. Injection volume was 2 μL and flow rate was 400 μL/min in both cases. The mass spectrometric conditions are described elsewhere (Krakkó et al., 2019). The total organic carbon (TOC) content was determined in the form of non-purgeable organic carbon using a Multi N/C 2100 S TC-TN analyzer (Analytik Jena, Jena, Germany).

3. Results and discussion

3.1. Removal kinetics of tetracycline

Degradation rate of tetracycline was evaluated under UV and (V) UV irradiation in the absence (referred to as photolysis) and presence of dissolved oxygen (referred to as photooxidation) (Fig. 1A). As expected, the effect of (V)UV irradiation drastically increased the degradation rate of TETR compared to UV irradiation (Table 1.) as it has been previously demonstrated for TETR and other APIs (Krakkó et al., 2019; Krakkó et al., 2022; Yao et al., 2017). Eleven and twelve-fold increase was observed between UV and (V)UV irradiation for photolysis and photooxidation, respectively. It is important to emphasize that although the lamp geometry was identical for the UV and (V)UV lamps, the total photon flux was approximately 18 times smaller for the (V)UV lamp in these experiments. The increased degradation rates in (V)UV experiments were due to the photodissociation of water induced by the vacuum UV photons, generating reactive species such as H_3O^+ , H^+ and hydrated electrons (e_{aq}^-) and most importantly, hydroxyl radicals (Krakkó et al., 2022; Yao et al., 2017). Moreover, vacuum UV photons could increase the degradation rate of TETR by direct photolytic cleavage. The effect of dissolved oxygen was minor, 9% and 16% increase could be observed in the case of UV and (V)UV irradiation, respectively. Dissolved oxygen can contribute to increased reaction rates through the formation of reactive oxidative species such as hydroperoxyl, peroxy or superoxide anion radicals. (Krakkó et al., 2022). Moreover, ozone could be generated in (V)UV photooxidation experiments following the photolysis of an oxygen molecule and recombination of the formed oxygen atom with another oxygen molecule (Krakkó et al., 2022). Additionally, oxygen can hinder the recombination reaction of hydrogen atoms and hydroxyl radicals generated during irradiation and thus increase the concentration of hydroxyl radicals in the solution compared to photolysis experiments conducted in the absence of oxygen (Kozmér et al., 2016). The degradation rate-accelerating effect of dissolved oxygen and ozone in (V)UV irradiation depends on the photon flux at 185 nm of the (V)UV lamp. The concentration of hydroxyl radicals in the solution will increase with higher photon flux, and consequently, the effect of ozone, and the reactive oxidative

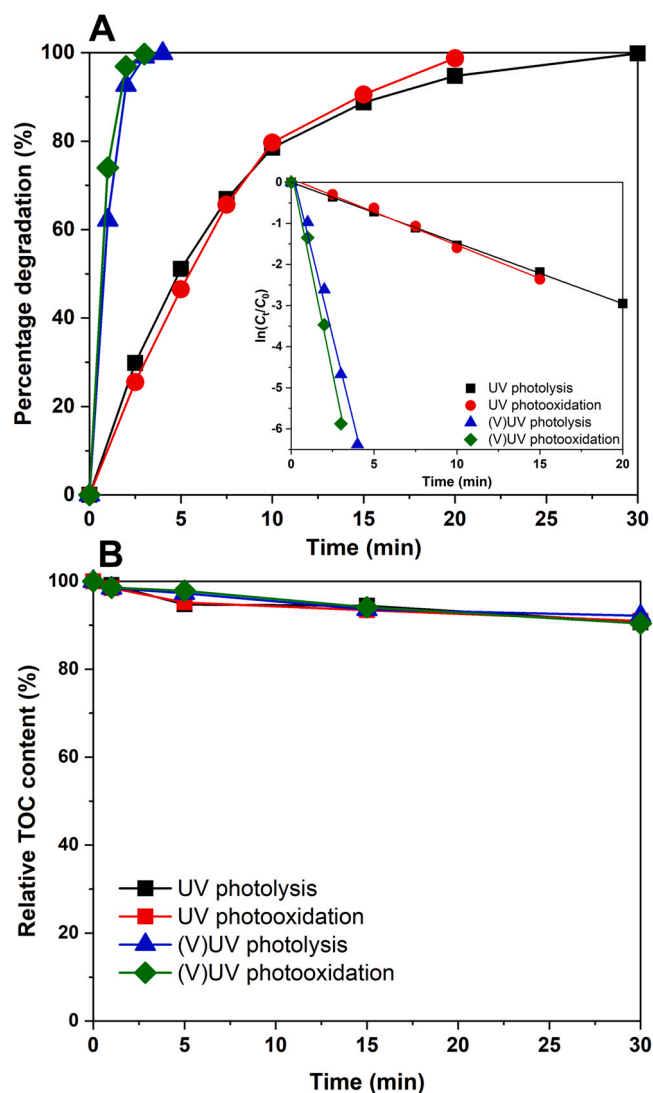


Fig. 1. Percentage degradation and linear regressions of tetracycline (A) and mineralization of tetracycline (B) as a function of irradiation time under different experimental conditions.

species generated in secondary reactions that involve dissolved oxygen will be negligible. TOC removal was less than 10% for UV photolysis and UV photooxidation (Fig. 1B), dissolved oxygen did not play a significant role in the mineralization in this case because no difference could be observed for UV photolysis and UV photooxidation.

Similar results were observed in (V)UV experiments as in UV experiments. This meant 10% decrease in TOC content in 30 min irradiation time (Fig. 1B). On the other hand, with a photon flux increased by 18 times (achieved by removing the Pyrex covers from the top and bottom of the (V)UV lamp), high TOC removal of 80% was reached in (V)UV photooxidation experiments, similarly to another study (Yao et al., 2017), and to other APIs discussed elsewhere (Krakkó et al., 2019; Krakkó et al., 2021).

3.2. Transformation products of tetracycline

In total, 11 TPs were identified across all experimental conditions (Table 2 and Table S1). According to the MS² spectrum, TETR (Fig. S1) during fragmentation undergoes losses of ammonia (m/z 445.16 → m/z 428.13), water (m/z 428.13 → m/z 410.12 → m/z 392.11) and CO (m/z 365.06 → m/z 337.07; m/z 297.07 → m/z 269.08 → m/z 241.08;

Table 1
Kinetic parameters for UV and (V)UV degradation of tetracycline under different experimental conditions.

	UV irradiation		(V)UV irradiation	
	Photolysis	Photooxidation	Photolysis	Photooxidation
$t_{1/2}$ (s)	281.8 ± 3.6	256.7 ± 10.4	25.27 ± 1.7	21.07 ± 1.8
k (10^{-3} s $^{-1}$)	2.46 ± 0.03	2.70 ± 0.11	27.43 ± 1.8	32.90 ± 2.8

Abbreviations: k = pseudo-first order rate constant, $t_{1/2}$ = half-life. Two sigma limits were used for error calculations.

m/z 126.05 → m/z 98.06) and the dimethylamine group (m/z 410.12 → m/z 365.06).

TP 460 is the hydroxylated product of TETR. Two isomeric peaks (Fig. S2) with different retention time could be identified as reported also by others (Wan et al., 2013; Zhang et al., 2018). The exact place of the new hydroxyl group could not be determined by mass spectrometry but according to Liang et al., the C11a position (Fig. 2, Ring C) is the most vulnerable for hydroxyl radical attack that is followed by oxo-enol tautomerization (Liang et al., 2018). Other possible sites for hydroxyl radical attack are C7–9 positions on the D phenyl ring of TETR (Fig. 2).

Based on its exact mass, TP 458 contains one oxygen atom more and two hydrogen atoms less compared to TETR (Fig. S3). TP 458 could only be detected in (V)UV experiments. According to the literature, TP 458 was formed by hydrogen abstraction from TP 460 initiated by the consecutive attack of a hydroxyl radical and an oxygen atom or another radical species (Ao et al., 2019; Li and Hu, 2016).

The difference between the molecular formula of TP 442 and TETR is two hydrogen atoms (Fig. S4). It was proposed that TP 442 formed from TP 460 by dehydration (water loss) in position C6 (Ao et al., 2019; Liu et al., 2016). Similarly to TP 458, TP 442 was only detected in (V)UV experiments.

TP 430 is a demethylated product of TETR likely formed in direct photolytic reaction (Fig. S5). There were two possible positions for demethylation in the structure of TETR, either at C6 position or at the dimethylamine group of TETR. It is argued that cleavage at the dimethylamine group is favored due to the low bond energy of the N–C bond (Jiao et al., 2008; Li and Hu, 2016). This was confirmed in our study by high resolution MS² measurements. A characteristic fragment ion of TETR is m/z 154.05 that was produced by a loss of the primer amino group and the fragmentation of the main structure in two parts (Fig. S6). This fragment ion was characteristic for the dimethylamine group of the molecule. A similar fragment ion could be observed for TP 430 with the difference of a methyl group according to the exact mass of this fragment ion, confirming that demethylation of TETR took place on the dimethylamine group to form TP 430 (Fig. S5).

TP 426 (Fig. S7) was a dehydrated TP of TETR likely produced via direct photoelimination of water as it was present in each type of experiments including UV photolysis (Table S1). It is believed that water loss took place at the C6 position and was followed by oxo-enol tautomerism to form a more stable structure containing a second aromatic ring (Halling-Sørensen et al., 2002; Liu et al., 2016).

The structure of TP 418 could not be clarified based solely on the mass spectrometric data (Fig. S8). To the best of our knowledge, this product was not yet described in the literature. According to its exact mass, the unequivocal molecular formula of its protonated molecule is C₂₁H₂₇N₂O₇. TP 418 was only detected in (V)UV experiments.

TETR can undergo photochemical decarbonylation to form TP 416 (Fig. S9). There are two possible positions for the decarbonylation, namely C1 and C11. According to the literature, bond cleavage could occur in acetylacetone molecules by high energy UV irradiation (Upadhyaya et al., 2003). Acetylacetone exists predominantly in enolic form (Upadhyaya et al., 2003), thus position C1 was more likely for the decarbonylation because of the enolic acetylacetone moiety in ring A of TETR (Fig. 2) (Ao et al., 2019). This hypothesis was

supported in our experiments by the proposed structure of some fragment ions of TP 416 (Fig. S10).

There were two possible routes for the formation of TP 412 (Fig. S11). It was either formed from TP 430 by dehydration similarly to the generation of TP 426 or through demethylation of TP 426. In the former case, water loss at position C6 was proposed to be followed by oxo-enol tautomerism. The formation of TP 412 from TP 430 was also confirmed by MS² measurements; among several identical fragment ions, fragment ion m/z 140.03 indicated that TP 412 was missing a methyl group from the dimethylamine moiety of TETR as discussed earlier for TP 430. TP 412 was only detected in photolysis experiments.

TP 399 (Fig. S12) was formed from either TP 430 or TETR by direct photoelimination of the methylamino or dimethylamine group, respectively. TP 399 was only detected in photolysis experiments. Transformation products with the same nominal mass have been described previously, indicating losses of two methyl and a hydroxyl group (Cao et al., 2016) or a methyl, the primer amino and a hydroxyl group (Zhu et al., 2013). In those studies, low resolution mass spectrometry was applied. In our case, the only possible molecular formula based on high resolution mass spectrometry with a mass accuracy limit of 10 ppm indicated a loss of “C₂H₈N” that corresponded to the loss of the dimethylamine group.

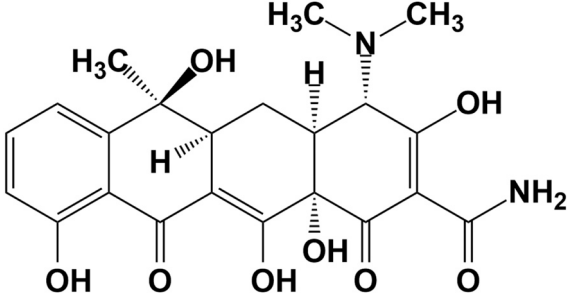
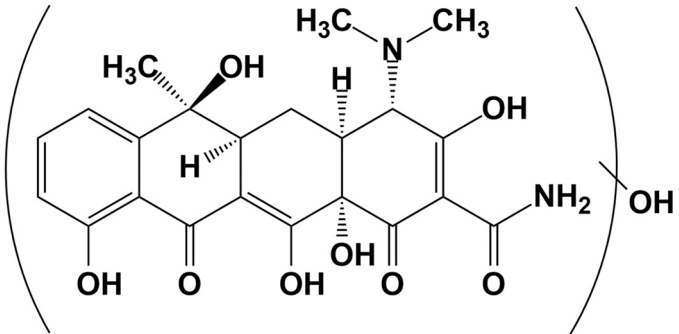
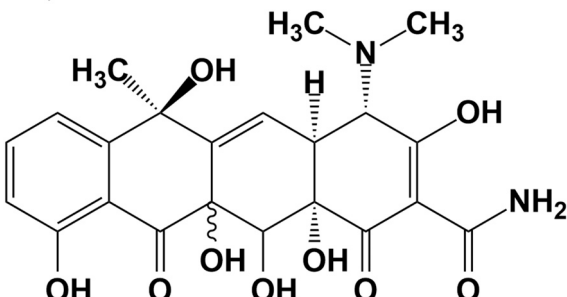
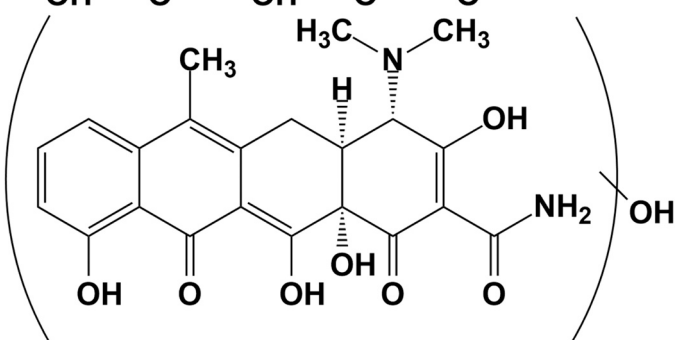
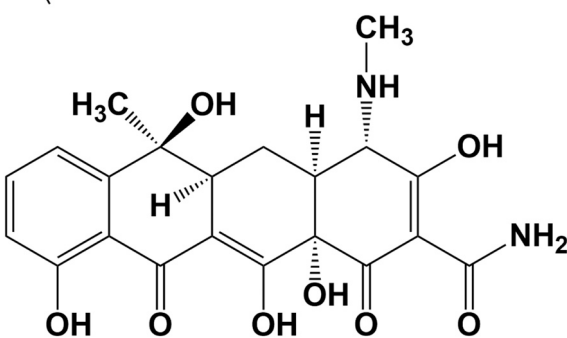
TP 398 (Fig. S13) was a newly identified transformation product of TETR. It was possibly generated from TP 426 by decarbonylation or from TP 416 by dehydration. After dehydration, the same oxo-enol tautomerism was proposed as discussed earlier. The MS² spectra of these three TPs served as a confirmation of their similar structures. Firstly, TP 398 and TP 416 shared several fragment ions (m/z 382.13, m/z 364.12, m/z 311.09, m/z 293.08 and m/z 237.05). Secondly, the mass difference between several fragment ions of TP 426 and TP 398 was equal to the loss of a CO (m/z 410.12 of TP 426 → m/z 382.13 of TP 398, m/z 392.11 of TP 426 → m/z 364.12 of TP 398 and m/z 321.07 of TP 426 → m/z 293.08 of TP 398).

TP 383 was another newly identified transformation product of TETR (Fig. S14). The exact mechanism of its formation is unknown, but it involved the loss of the dimethylamine group and the loss of a hydroxyl group (not water loss according to the exact masses). We hypothesize that the hydroxyl group was lost from the C3 carbon atom that is adjacent to the carbon atom with the dimethylamine group (Fig. 2).

Based on the identified TPs, both direct photolytic reactions and reactions with radical species were involved in the degradation of TETR (Fig. 2) under UV and (V)UV light. According to the proposed mechanism, TETR can be oxidized to TP 460 upon hydroxyl radical attack. TETR can also suffer loss of CO (TP 416), a methyl group (TP 430) or the dimethylamine group (TP 383) or loss of H₂O can take place (TP 426). In further steps, the same degradation reaction steps are repeated and TPs with smaller molecular weight are formed; in our experiments, loss of H₂O was observed in the case of several TPs (TP 416 → TP 398, TP 460 → TP 442, TP 430 → TP 412), as well as a loss of CO (TP 426 → TP 398), a loss of a methyl group (TP 426 → TP 412) or the loss of the methylamino group (TP 430 → TP 399). Moreover, the exact formation of TP 418 and TP 383 is unknown.

As none of the identified TPs were characteristic for ozonation reactions, it is more likely that the ozone generated in (V)UV experiments was degraded by (V)UV light to O(¹D) and an oxygen

Table 2
Transformation products of tetracycline identified during UV and (V)UV irradiation.

Name and molecular formula [M+H ⁺]	Retention time (min)	Accurate mass [M+H ⁺] (mass accuracy)	DBE [M+H] ⁺	Structure	Confidence level ^a
TETR C ₂₂ H ₂₅ N ₂ O ₈	5.2	445.1602 (-0.8)	11.5		1
TP 460 C ₂₂ H ₂₅ N ₂ O ₉	1.8, 3.3	461.1546 (-1.9)	11.5		3
TP 458 C ₂₂ H ₂₃ N ₂ O ₉	7.8	459.1381 (3.7)	12.5		3
TP 442 C ₂₂ H ₂₃ N ₂ O ₈	11.3	443.1432 (3.8)	12.5		3
TP 430 C ₂₁ H ₂₃ N ₂ O ₈	4.8	431.1452 (-0.7)	11.5		2

(continued on next page)

Table 2 (continued)

Name and molecular formula [M+H ⁺]	Retention time (min)	Accurate mass [M+H ⁺] (mass accuracy)	DBE [M+H ⁺] ^a	Structure	Confidence level ^a
TP 426 C ₂₂ H ₂₃ N ₂ O ₇	10.5	427.1506 (-1.5)	12.5		3
TP 418 C ₂₁ H ₂₇ N ₂ O ₇	6.2	419.1805 (1.9)	9.5	unknown	4
TP 416 C ₂₁ H ₂₅ N ₂ O ₇	5.6	417.1662 (-1.4)	10.5		3
TP 412 C ₂₁ H ₂₁ N ₂ O ₇	9.9	413.1338 (1.3)	12.5		3
TP 399 C ₂₀ H ₁₈ NO ₈	9.6	400.1021 (1.5)	12.5		2
TP 398 C ₂₁ H ₂₃ N ₂ O ₆	5.1	399.1559 (-2.1)	11.5		3

(continued on next page)

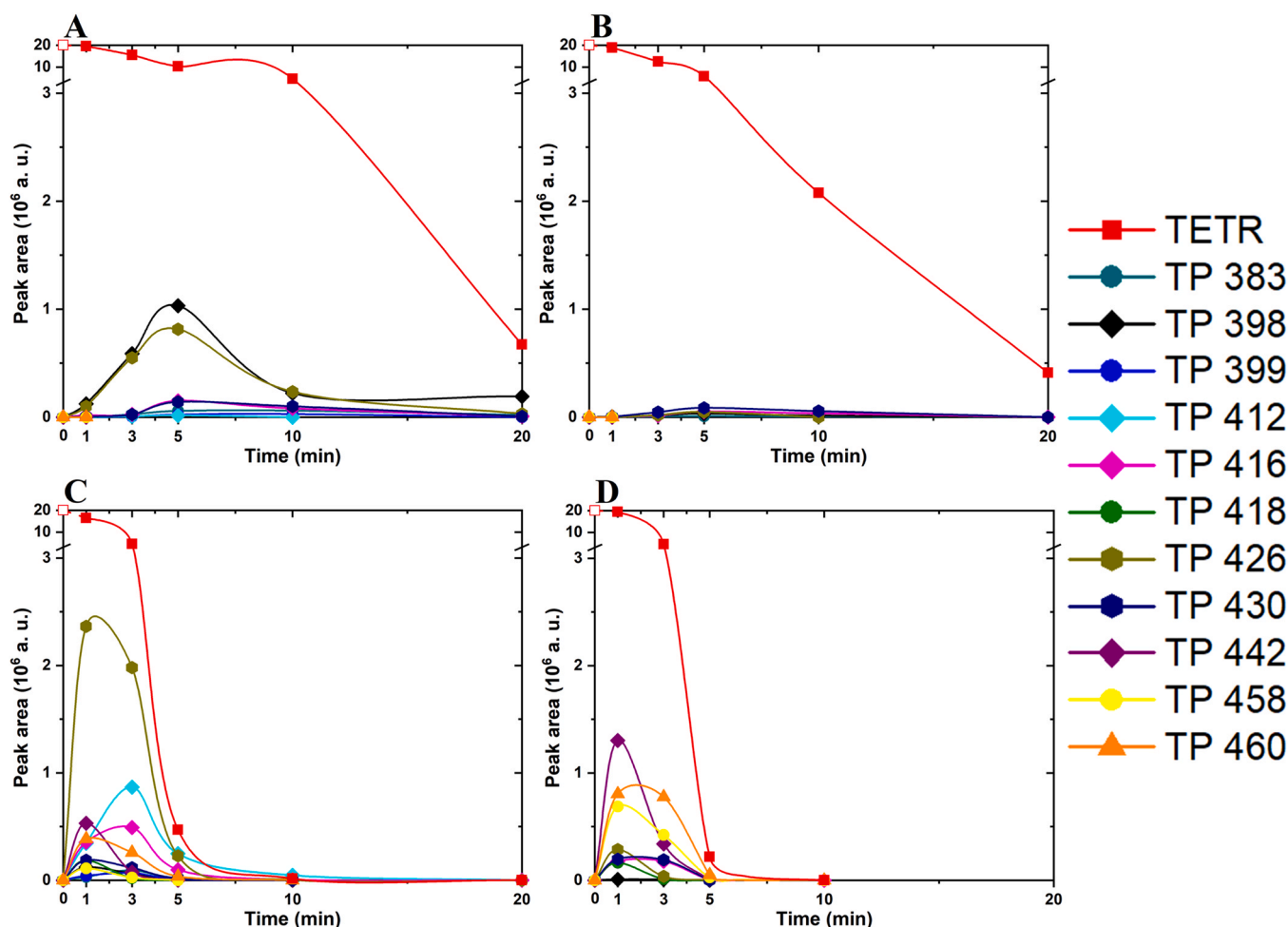


Fig. 3. Kinetic profile of the transformation products of tetracycline during UV photolysis (A), UV photooxidation (B), (V)UV photolysis (C), and (V)UV photooxidation (D) in ultrapure water.

molecule, and ultimately contributed to the generation of hydroxyl radicals via the reaction of $O(^1D)$ with water. Dissolved ozone could also react with water under UV light to generate H_2O_2 . Photolytic degradation of H_2O_2 , or its reaction with ozone will also form hydroxyl radicals (Krakkó et al., 2021).

3.3. Kinetic profile of the transformation products of tetracycline

Although the main TPs of TETR were the same in each type of experiment, the kinetic profiles were different (Fig. 3). The dominant degradation route for TETR in UV photolysis was $TETR \rightarrow TP\ 426 \rightarrow TP\ 398$, and eight out of eleven TPs could be detected in total (see Table S1). In the case of UV photolysis, reactive oxidative species are generated in secondary photochemical reactions and degradation is mainly driven by direct photolytic reactions. Similarly to UV photolysis, TP 426 was also the dominant TP in (V)UV photolysis. However, the kinetic profile of TP 398 did not follow TP 426 in (V)UV experiments, indicating that TP 426 was more likely hydroxylated or demethylated in this case. Three compounds, namely TP 458, TP 442 and TP 418 were only detected in (V)UV experiments. This could be explained by the higher concentration of hydroxyl ions in (V)UV experiments or higher photon flux that favored their formation in detectable amounts.

Only 5 TPs could be detected in total in UV photooxidation experiments and a dominant path could not be identified. Three TPs, namely TP 412, TP 399 and TP 383 could not be detected when oxygen was present in the samples. This indicated that other

pathways were favored in the presence of oxygen. It can be assumed that the rate-determining step in the formation of these TPs was reactions with UV or VUV photons. These reactions took place through excited states of TETR and TP 430. These excited states could be effectively quenched by oxygen molecules. Consequently, direct photolysis with VUV photons, and reactions with reactive oxidative species (most importantly hydroxyl radicals) were the most dominant in (V)UV photooxidation that is in accordance with the highest TOC removal for this treatment type.

4. Conclusions

Three new TPs for the (V)UV degradation of TETR could be identified, namely TP 418, TP 398 and TP 383, and structure was proposed for two out of three TPs. The degradation rate of TETR and its aromatic TPs could be drastically increased by applying (V)UV irradiation compared to the conventional “germicidal” UV treatment. The number of identified TPs was also less in case of (V)UV experiments that indicated that the aromatic TPs were more efficiently mineralized, or transformed into smaller compounds. (V)UV irradiation could effectively remove the identified TPs within 10 min irradiation time. Degradation pathways involving reactive oxidative species is hypothesized to be more relevant in wastewater applications as photons will more likely react with water or matrix components of the wastewater.

CRedit authorship contribution statement

Dániel Krakkó: Investigation, Writing – original draft, Visualization. **Bjørn Tobiassen Heieren:** Investigation, Writing – original draft, Visualization. **Ádám Illés:** Investigation, Writing – original draft, Visualization. **Kristin Kvamme:** Supervision. **Sándor Dóbbé:** Supervision, Writing – review & editing. **Gyula Záray:** Funding acquisition, Writing – review & editing.

Declaration of Competing Interest

The authors declare that they have no known competing financial interests or personal relationships that could have appeared to influence the work reported in this paper.

Acknowledgment

This work was supported by the National Research Development and Innovation Office of Hungary [grant number NVKP_16-1-2016-0045].

Appendix A. Supporting information

Supplementary data associated with this article can be found in the online version at [doi:10.1016/j.psep.2022.05.027](https://doi.org/10.1016/j.psep.2022.05.027).

References

- Alharbi, O.M.L., Basheer, A.A., Khattab, R.A., Ali, I., 2018. Health and environmental effects of persistent organic pollutants. *J. Mol. Liq.* 263, 442–453. <https://doi.org/10.1016/j.molliq.2018.05.029>
- Ao, X., Sun, W., Li, S., Yang, C., Li, C., Lu, Z., 2019. Degradation of tetracycline by medium pressure UV-activated peroxymonosulfate process: Influencing factors, degradation pathways, and toxicity evaluation. *Chem. Eng. J.* 361, 1053–1062. <https://doi.org/10.1016/j.cej.2018.12.133>
- Aus der Beek, T., Weber, F.A., Bergmann, A., Hickmann, S., Ebert, I., Hein, A., Küster, A., 2016. Pharmaceuticals in the environment—global occurrences and perspectives. *Environ. Toxicol. Chem.* 35 (4), 823–835. <https://doi.org/10.1002/etc.3339>
- Cao, M., Wang, P., Ao, Y., Wang, C., Hou, J., Qian, J., 2016. Visible light activated photocatalytic degradation of tetracycline by a magnetically separable composite photocatalyst: graphene oxide/magnetite/cerium-doped titania. *J. Colloid Interface Sci.* 467, 129–139. <https://doi.org/10.1016/j.jcis.2016.01.005>
- Emzhina, V., Kuzin, E., Babusenko, E., Krutchinina, N., 2021. Photodegradation of tetracycline in presence of H₂O₂ and metal oxide based catalysts. *J. Water Process Eng.* 39, 101696. <https://doi.org/10.1016/j.jwpe.2020.101696>
- European Commission, 2019. European union Strategic Approach to Pharmaceuticals in the Environment: Communication from the Commission to the European Parliament, the Council and the European Economic and Social Committee. COM, 128.
- Ghadim, E.E., Manouchehri, F., Soleimani, G., Hosseini, H., Kimiagar, S., Nafisi, S., 2013. Adsorption properties of tetracycline onto graphene oxide: equilibrium, kinetic and thermodynamic studies. *PLOS ONE* 8 (11), e79254. <https://doi.org/10.1371/journal.pone.0079254>
- Granados-Chinchilla, F., Rodríguez, C., 2017. Tetracyclines in food and feedstuffs: from regulation to analytical methods, bacterial resistance, and environmental and health implications. *J. Anal. Methods Chem.* 2017, 1315497. <https://doi.org/10.1155/2017/1315497>
- Guo, X., Yan, Z., Zhang, Y., Xu, W., Kong, D., Shan, Z., Wang, N., 2018. Behavior of antibiotic resistance genes under extremely high-level antibiotic selection pressures in pharmaceutical wastewater treatment plants. *Sci. Total Environ.* 612, 119–128. <https://doi.org/10.1016/j.scitotenv.2017.08.229>
- Halling-Sørensen, B., Sengeløv, G., Tjørnelund, J., 2002. Toxicity of tetracyclines and tetracycline degradation products to environmentally relevant bacteria, including selected tetracycline-resistant bacteria. *Arch. Environ. Contam. Toxicol.* 42 (3), 263–271. <https://doi.org/10.1007/s00244-001-0017-2>
- Huizar-Félix, A.M., Aguilar-Flores, C., Martínez-de-la Cruz, A., Barandiarán, J.M., Sepúlveda-Guzmán, S., Cruz-Silva, R., 2019. Removal of tetracycline pollutants by adsorption and magnetic separation using reduced graphene oxide decorated with α -Fe₂O₃ nanoparticles. *Nanomaterials* 9 (3), 313. <https://doi.org/10.3390/nano9030313>
- Jiao, S., Zheng, S., Yin, D., Wang, L., Chen, L., 2008. Aqueous photolysis of tetracycline and toxicity of photolytic products to luminescent bacteria. *Chemosphere* 73 (3), 377–382. <https://doi.org/10.1016/j.chemosphere.2008.05.042>
- Kozmér, Z., Arany, E., Alapi, T., Rózsá, G., Hernádi, K., Dombi, A., 2016. New insights regarding the impact of radical transfer and scavenger materials on the OH-initiated phototransformation of phenol. *J. Photochem. Photobiol. A Chem.* 314, 125–132. <https://doi.org/10.1016/j.jphotochem.2015.08.023>
- Krakkó, D., Gombos, E., Licul-Kucera, V., Dóbbé, S., Mihucz, V.G., Záray, G., 2019. Enhanced photolytic and photooxidative treatments for removal of selected pharmaceutical ingredients and their degradation products in water matrices. *Microchem. J.* 150, 104136. <https://doi.org/10.1016/j.microc.2019.104136>
- Krakkó, D., Illés, Á., Domján, A., Demeter, A., Dóbbé, S., Záray, G., 2022. UV and (V)UV irradiation of sitagliptin in ultrapure water and WWTP effluent: kinetics, transformation products and degradation pathway. *Chemosphere* 288, 132393. <https://doi.org/10.1016/j.chemosphere.2021.132393>
- Krakkó, D., Illés, Á., Licul-Kucera, V., Dávid, B., Dobosy, P., Pogonyi, A., Demeter, A., Mihucz, V.G., Dóbbé, S., Záray, G., 2021. Application of (V)UV/O₃ technology for post-treatment of biologically treated wastewater: a pilot-scale study. *Chemosphere* 275, 130080. <https://doi.org/10.1016/j.chemosphere.2021.130080>
- Li, S., Hu, J., 2016. Photolytic and photocatalytic degradation of tetracycline: effect of humic acid on degradation kinetics and mechanisms. *J. Hazard. Mater.* 318, 134–144. <https://doi.org/10.1016/j.jhazmat.2016.05.100>
- Li, S., Xue, B., Chen, J., Liu, Y., Zhang, J., Wang, H., Liu, J., 2021. Constructing a plasmonic p-n heterojunction photocatalyst of 3D Ag/Ag₆Si₂O₇/Bi₂MoO₆ for efficiently removing broad-spectrum antibiotics. *Sep. Purif. Technol.* 254, 117579. <https://doi.org/10.1016/j.seppur.2020.117579>
- Liang, S., Lin, H., Yan, X., Huang, Q., 2018. Electro-oxidation of tetracycline by a Magnéli phase Ti₄O₇ porous anode: Kinetics, products, and toxicity. *Chem. Eng. J.* 332, 628–636. <https://doi.org/10.1016/j.cej.2017.09.109>
- Liu, H., Xu, G., Li, G., 2021. Preparation of porous biochar based on pharmaceutical sludge activated by NaOH and its application in the adsorption of tetracycline. *J. Colloid Interface Sci.* 587, 271–278. <https://doi.org/10.1016/j.jcis.2020.12.014>
- Liu, X., Guo, X., Liu, Y., Lu, S., Xi, B., Zhang, J., Wang, Z., Bi, B., 2019. A review on removing antibiotics and antibiotic resistance genes from wastewater by constructed wetlands: Performance and microbial response. *Environ. Pollut.* 254, 112996. <https://doi.org/10.1016/j.envpol.2019.112996>
- Liu, Y., He, X., Fu, Y., Dionysiou, D.D., 2016. Kinetics and mechanism investigation on the destruction of oxytetracycline by UV-254nm activation of persulfate. *J. Hazard. Mater.* 305, 229–239. <https://doi.org/10.1016/j.jhazmat.2015.11.043>
- Loos, R., Marinov, D., Sanseverino, I., Napierska, D., Lettieri, T., 2018. Review of the 1st watch list under the water framework directive and recommendations for the 2nd watch list. *Publ. Off. Eur. Union.* <https://doi.org/10.2760/614367>
- Luu, H.T., Lee, K., 2014. Degradation and changes in toxicity and biodegradability of tetracycline during ozone/ultraviolet-based advanced oxidation. *Water Sci. Technol.* 70 (7), 1229–1235. <https://doi.org/10.2166/wst.2014.350>
- Mao, W., Zhang, L., Wang, T., Bai, Y., Guan, Y., 2021. Fabrication of highly efficient Bi₂WO₆/CuS composite for visible-light photocatalytic removal of organic pollutants and Cr(VI) from wastewater. *Front. Environ. Sci. Eng.* 15 (4), 52. <https://doi.org/10.1007/s11783-020-1344-8>
- Michael, I., Rizzo, L., McArdell, C.S., Manaia, C.M., Merlin, C., Schwartz, T., Dagot, C., Fatta-Kassinos, D., 2013. Urban wastewater treatment plants as hotspots for the release of antibiotics in the environment: a review. *Water Res.* 47 (3), 957–995. <https://doi.org/10.1016/j.watres.2012.11.027>
- Roudbari, A., Rezakazemi, M., 2018. Hormones removal from municipal wastewater using ultrasound. *AMB Express* 8 (1), 91. <https://doi.org/10.1186/s13568-018-0621-4>
- Schymanski, E.L., Jeon, J., Gulde, R., Fenner, K., Ruff, M., Singer, H.P., Hollender, J., 2014. Identifying small molecules via high resolution mass spectrometry: communicating confidence. *Environ. Sci. Technol.* 48 (4), 2097–2098. <https://doi.org/10.1021/es5002105>
- Segura, P.A., François, M., Gagnon, C., Sauvée, S., 2009. Review of the occurrence of anti-infectives in contaminated wastewaters and natural and drinking waters. *Environ. Health Perspect.* 117 (5), 675–684. <https://doi.org/10.1289/ehp.11776>
- Upadhyaya, H.P., Kumar, A., Naik, P.D., 2003. Photodissociation dynamics of enolic-acetylacetone at 266, 248, and 193 nm: Mechanism and nascent state product distribution of OH. *J. Chem. Phys.* 118 (6), 2590–2598. <https://doi.org/10.1063/1.1535424>
- Wan, Y., Jia, A., Zhu, Z., Hu, J., 2013. Transformation of tetracycline during chloramination: kinetics, products and pathways. *Chemosphere* 90 (4), 1427–1434. <https://doi.org/10.1016/j.chemosphere.2012.09.001>
- Wu, S., Hu, H., Lin, Y., Zhang, J., Hu, Y.H., 2020. Visible light photocatalytic degradation of tetracycline over TiO₂. *Chem. Eng. J.* 382, 122842. <https://doi.org/10.1016/j.cej.2019.122842>
- Wu, S., Li, X., Tian, Y., Lin, Y., Hu, Y.H., 2021. Excellent photocatalytic degradation of tetracycline over black anatase-TiO₂ under visible light. *Chem. Eng. J.* 406, 126747. <https://doi.org/10.1016/j.cej.2020.126747>
- Xu, L., Zhang, H., Xiong, P., Zhu, Q., Liao, C., Jiang, G., 2021. Occurrence, fate, and risk assessment of typical tetracycline antibiotics in the aquatic environment: a review. *Sci. Total Environ.* 753, 141975. <https://doi.org/10.1016/j.scitotenv.2020.141975>
- Xu, M., Deng, J., Cai, A., Ma, X., Li, J., Li, Q., Li, X., 2020. Comparison of UVC and UVC/persulfate processes for tetracycline removal in water. *Chem. Eng. J.* 384, 123320. <https://doi.org/10.1016/j.cej.2019.123320>
- Yang, S., Carlson, K., 2003. Evolution of antibiotic occurrence in a river through pristine, urban and agricultural landscapes. *Water Res.* 37 (19), 4645–4656. [https://doi.org/10.1016/s0043-1354\(03\)00399-3](https://doi.org/10.1016/s0043-1354(03)00399-3)
- Yao, H., Pei, J., Wang, H., Fu, J., 2017. Effect of Fe(II/III) on tetracycline degradation under UV/VUV irradiation. *Chem. Eng. J.* 308, 193–201. <https://doi.org/10.1016/j.cej.2016.09.074>
- Yin, H., Cao, Y., Fan, T., Zhang, M., Yao, J., Li, P., Chen, S., Liu, X., 2021. In situ synthesis of Ag₃PO₄/C₃N₅ Z-scheme heterojunctions with enhanced visible-light-responsive photocatalytic performance for antibiotics removal. *Sci. Total Environ.* 754, 141926. <https://doi.org/10.1016/j.scitotenv.2020.141926>

Zhang, Y., Shi, J., Xu, Z., Chen, Y., Song, D., 2018. Degradation of tetracycline in a solar/H₂O₂ system: proposed mechanism and intermediates. *Chemosphere* 202, 661–668. <https://doi.org/10.1016/j.chemosphere.2018.03.116>

Zhao, T., Zheng, M., Fu, C., Li, G., Xiong, Y., Qiu, W., Zhang, T., Zhang, J., Zheng, C., 2020. Effect of low-level H₂O₂ and Fe(II) on the UV treatment of tetracycline antibiotics

and the toxicity of reaction solutions to zebrafish embryos. *Chem. Eng. J.* 394, 125021. <https://doi.org/10.1016/j.cej.2020.125021>

Zhu, X.-D., Wang, Y.-J., Sun, R.-J., Zhou, D.-M., 2013. Photocatalytic degradation of tetracycline in aqueous solution by nanosized TiO₂. *Chemosphere* 92 (8), 925–932. <https://doi.org/10.1016/j.chemosphere.2013.02.066>